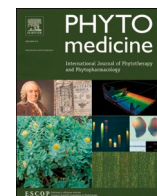




Since January 2020 Elsevier has created a COVID-19 resource centre with free information in English and Mandarin on the novel coronavirus COVID-19. The COVID-19 resource centre is hosted on Elsevier Connect, the company's public news and information website.

Elsevier hereby grants permission to make all its COVID-19-related research that is available on the COVID-19 resource centre - including this research content - immediately available in PubMed Central and other publicly funded repositories, such as the WHO COVID database with rights for unrestricted research re-use and analyses in any form or by any means with acknowledgement of the original source. These permissions are granted for free by Elsevier for as long as the COVID-19 resource centre remains active.



Discovery of *Camellia sinensis* catechins as SARS-CoV-2 3CL protease inhibitors through molecular docking, intra and extra cellular assays

Shi-Yu Liu^{a,1}, Wei Wang^{a,c,1}, Jia-Ping Ke^a, Peng Zhang^a, Gang-Xiu Chu^{b,*}, Guan-Hu Bao^{a,*}

^a Natural Products Laboratory, State Key Laboratory of Tea Plant Biology and Utilization, Anhui Agricultural University, Hefei, People's Republic of China

^b School of information and computer, Anhui Agricultural University, Hefei, People's Republic of China

^c Anhui Engineering Laboratory for Conservation and Sustainable Utilization of Traditional Chinese Medicine Resources, West Anhui University, Lu'an, 237000, China

ARTICLE INFO

Keywords:

(-)-epicatechin 3-O-caffeate
catechins
Camellia sinensis
SARS-CoV-2
ebiselen

ABSTRACT

Background and purpose: Previous studies suggest that major *Camellia sinensis* (tea) catechins can inhibit 3-chymotrypsin-like cysteine protease (3CLpro), inspiring us to study 3CLpro inhibition of the recently discovered catechins from tea by our group.

Methods: Autodock was used to dock 3CLpro and 16 tea catechins. Further, a 3CLpro activity detection system was used to test their intra and extra cellular 3CLpro inhibitory activity. Surface plasmon resonance (SPR) was used to analyze the dissociation constant (K_D) between the catechins and 3CLpro.

Results: Docking data suggested that 3CLpro interacted with the selected 16 catechins with low binding energy through the key amino acid residues Thr24, Thr26, Asn142, Gly143, His163, and Gln189. The selected catechins other than zizuanin D (3) and (-)-8-(5'-R)-N-ethyl-2-pyrrolidinone-3-O-cinnamoylepicatechin (11) can inhibit 3CLpro intracellularly. The extracellular 3CLpro IC_{50} values of (-)-epicatechin 3-O-caffeate (EC-C, 1), zizuanin C (2), etc-pyrrolidinone C and D (6), etc-pyrrolidinone A (9), (+)-galliccatechin gallate (GCG), and (-)-epicatechin gallate (ECG) are 1.58 ± 0.21 , 41.2 ± 3.56 , 0.90 ± 0.03 , 46.71 ± 10.50 , 3.38 ± 0.48 , and 71.78 ± 8.36 μ M, respectively. The K_D values of 1, 6, and GCG are 4.29, 3.46, and 3.36 μ M, respectively.

Conclusion: Together, EC-C (1), etc-pyrrolidinone C and D (6), and GCG are strong 3CLpro inhibitors. Our results suggest that structural modification of catechins could be conducted by esterifying the 3-OH as well as changing the configuration of C-3, C-3'' or C-5''' to discover strong SARS-CoV-2 inhibitors.

Introduction

The novel coronavirus (severe acute respiratory syndrome coronavirus 2, SARS-CoV-2) has spread rapidly around the world and has become a global health emergency (Li et al., 2020). SARS-CoV-2 is an enveloped single-stranded RNA virus (Oberfeld et al., 2020). 3-Chymotrypsin-like cysteine protease (3CLpro) or main protease is one of the most important proteins of the virus, which has already been identified as an important pharmacological target in the severe acute respiratory coronavirus syndrome (SARS-CoV) and Middle East respiratory syndrome virus (MERS) viruses. This protein triggers the production of a whole series of enzymes necessary for the virus to carry out its

replicating and infectious activities. (Grottesi et al., 2020). Meanwhile, since a protease homologous to 3CLpro is not present in the human body, 3CLpro becomes an ideal anti-coronavirus target, which is responsible for processing polyproteins of nidoviruses and picornaviruses (Kim et al., 2016).

Camellia sinensis (L.) Kuntze (Theaceae) (common name 'tea') is normally classified into six major types (green tea, white tea, yellow tea, oolong tea, black tea, and dark tea) according to the processing manufacture, and is popularly consumed around the world (Ke et al. 2019). Green tea, black tea, and oolong tea were reported to inhibit the contagious virus SARS-CoV-2 dose-dependently by *in vitro* cell assays (Nishimura et al., 2021). Green tea can inhibit SARS-CoV-2 3CLpro with

Abbreviations: 3CLpro, 3-chymotrypsin-like cysteine protease; CG, (+)-catechin gallate; ECG, (-)-epicatechin gallate; EGCG, (-)-epigallocatechin gallate; ETFs, ester-type flavoalkaloids; GCG, (+)-galliccatechin gallate; Flu, Fluminescence; IC_{50} , half-maximal inhibitory concentration; K_D , dissociation constants; Luc, Luciferase; RLU, Renilla luminescence; SARS-CoV, severe acute respiratory syndrome coronavirus; SPR, Surface plasmon resonance.

* Corresponding authors Tel: +86-551-65786401. Fax: +86-551-65786765.

E-mail addresses: 31083@ahau.edu.cn (G.-X. Chu), baoguanhu@ahau.edu.cn (G.-H. Bao).

¹ Shi-Yu Liu and Wei Wang contributed equally to this work.

<https://doi.org/10.1016/j.phymed.2021.153853>

Received 17 July 2021; Received in revised form 26 October 2021; Accepted 6 November 2021

Available online 9 November 2021

0944-7113/© 2021 Elsevier GmbH. All rights reserved.

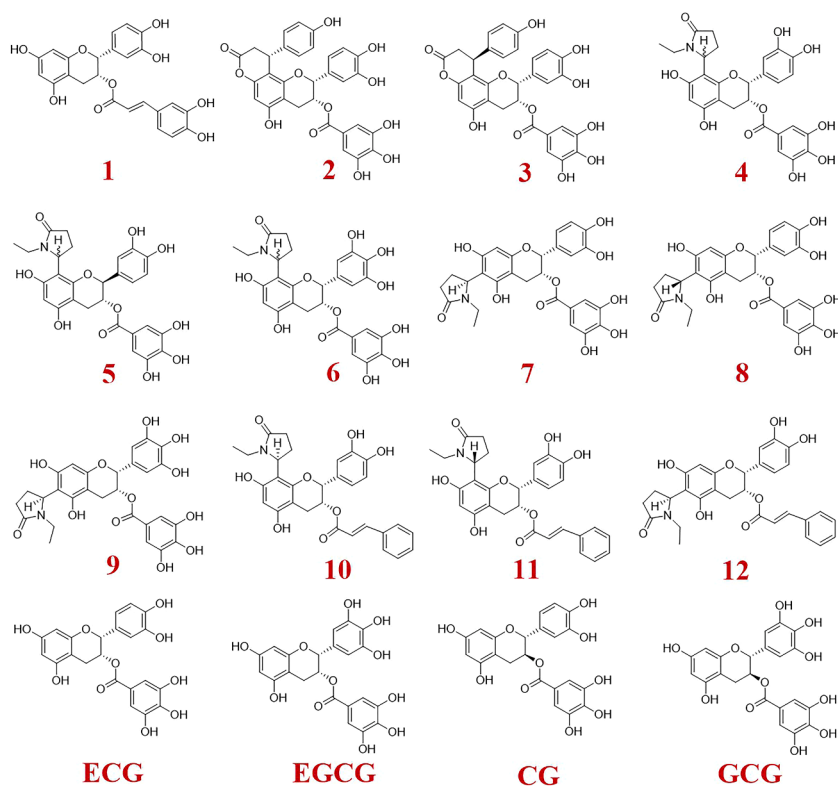


Fig. 1. Chemical structures of test catechins, (-)-epicatechin 3-O-cafфеoate (1), zijuannin C (2), zijuannin D (3), etc-pyrrolidinone G and H (4), etc-pyrrolidinone I and J (5), etc-pyrrolidinone C and D (6), etc-pyrrolidinone E (7), etc-pyrrolidinone F (8), etc-pyrrolidinone A (9), (-)-8-(5''S)-N-ethyl-2-pyrrolidinone-3-O-cinnamoylepicatechin (10), (-)-8-(5''R)-N-ethyl-2-pyrrolidinone-3-O-cinnamoylepicatechin (11), (-)-6-(5''S)-N-ethyl-2-pyrrolidinone-3-O-cinnamoylepicatechin (12), (-)-epicatechin gallate (ECG), (-)-epigallocatechin gallate (EGCG), (+)-catechin gallate (CG), and (+)-gallocatechin gallate (GCG).

a half-maximal inhibitory concentration (IC_{50}) at $8.9 \pm 0.5 \mu\text{g/ml}$ (Upadhyay et al., 2020). We used SARS-CoV-2 3CLpro for screening potential agents against the current fast epidemic since this protein has been used previously selected to screen anti-SARS-CoV-2 agents in silico and in vitro (Jang et al., 2021; Zhu and Xie, 2020). Common catechin monomers have high micromolar IC_{50} values while with *in vivo* concentrations of less than $1 \mu\text{M}$, searching for stronger catechins with small IC_{50} values is highly urgent and realizable for their utilization.

Researchers have found that introducing new chemical groups into the structure of catechins can significantly improve their stability and bioavailability, and specifically enhance their pharmacological effects (Liu et al., 2021; Xiao et al., 2013). Moreover, the effects of substitution at different positions are different. Thus, we selected 16 catechins (compounds 1–12), which had recently been isolated from tea by our group including the major tea catechins (-)-epigallocatechin gallate (EGCG), (-)-epicatechin gallate (ECG), (+)-catechin gallate (CG), and (+)-gallocatechin gallate (GCG) to test their 3CLpro inhibition activity. These catechins have previously demonstrated different biological activities. (-)-Epicatechin 3-O-cafфеoate (1, EC-C) can inhibit acetylcholinesterase activity (Wang et al., 2017), form complex with iron and neutrophil gelatinase-associated lipocalin, and protect against β -amyloid ($A\beta$) induced neurotoxicity in SH-SY5Y cells (Zhang et al., 2018). Zijuannin C (2) and zijuannin D (3) are catechin esters with impressive activity in protecting SH-SY5Y cells against H_2O_2 -induced damage (Ke et al., 2019). Compounds 4–9 are ester-type flavoalkaloids isolated from white tea (Bai-Mudan) and Chinese ancient cultivated tea (Xi-Gui), which can inhibit the accumulation of advanced glycation end products and cell senescence (Cheng et al., 2018; Li et al., 2018). Compounds 10–12 are four flavoalkaloid cinnamoyl esters with strong acetylcholinesterase inhibitory effects (Gaur et al., 2020).

Luciferase (Luc) refers to a class of enzymes that catalyze specific luciferin substrates to produce bioluminescence. Several luciferases require no post-translational processing for enzymatic activity and show

a linear relationship between concentration and their resulting bioluminescence (Wet et al., 1986). These properties render them excellent genetic reporters. Luc-fused proteins can be easily quantified by measuring their catalyzed bioluminescence with a luminometer, providing the detection sensitivity up to femtogram level (Williams et al., 1989). Luc biosensor system has the advantages of high sensitivity, ease of use, and applicability, which makes it a powerful tool for studying viral protease proteolysis events in living cells and achieving high-throughput screening of antiviral agents. Therefore, in this study, a cell-level screening model for the 3CLpro inhibitor of SARS-CoV-2 was established using a 3CLpro activity detection system. The intracellular detection system contains the following plasmids: a plasmid expressing 3CLpro substrate which carries renilla luc; a plasmid expressing 3CLpro; and a luc plasmid. A luc gene and a protein aggregation group gene are fused and expressed, and a 3CLpro enzyme peptide segment is arranged between the two genes. If the 3CLpro is cut at the peptide segment, the luc and the protein aggregation group are separated, leading to an active luc and a generated chemiluminescent light signal; conversely, when the 3Cpro activity is inhibited, a chemiluminescent signal is not generated. High-throughput screening and drug repurposing have suggested some potential hit compounds against SARS-CoV-2. People began to dock a set of bioactive molecules from tea plants with major proteins in SARS-CoV-2 and found some leading inhibitors against SARS-CoV-2 (Sharma et al., 2021). We screened the selected 16 catechins by molecular docking. Further, the extracellular IC_{50} values of 3CLpro of the selected active catechins were achieved. The substrate of 3CLpro has two fluorecent groups at both ends, one of which is a quenching group. When the substrate is not cut by 3CLpro, the substrate is quenched near fluorescence, and there is no fluorescence signal. When the substrate is separated by 3CLpro, a fluorescence signal will be generated. Finally, the binding K_D values of selected catechins and 3CLpro were determined by surface plasmon resonance (SPR) technology.

Materials and methods

Materials

Analytical grade reagents used for extraction and isolation were purchased from Chengdu Kelong Chemical Reagent Co., Ltd (Chengdu, China). CM7 sensor chip, 10 × PBS-P buffer (containing 0.2 M phosphate buffer, 27 mM and 1.37 M NaCl, 0.5% Surfactant P20, pH adjusted to yield pH 7.4 when diluted 10 × and supplemented with 2% DMSO), sodium acetate pH 4.0, 4.5, 5.0, 5.5 and amino coupling kit were purchased from Cytiva (Uppsala, Sweden). Dimethyl sulfoxide (DMSO) was purchased from Genthold (Beijing, China). 293T/17 cells (CBP6044) were purchased from Cobioer biosciences Co. Ltd (Nanjing, China). 3CLpro, plasmids expressing 3CLpro, and luc plasmid were provided by PreceDo Pharmaceuticals Co. Ltd (Hefei, China). 3CLpro activity

$$\%inhibition = 100 - (RLU\ compound / Flu\ compound) / (RLU\ control / Flu\ compound) * 100\%$$

detection system was purchased from Vazyme (Nanjing, China). DMEM medium was purchased from Corning (New York, NY, USA). Fetal bovine serum was purchased from Excell (Shanghai, China). EC-C (1), zijuanin C (2), zijuanins D (3), etc-pyrrolidinone G and H (4), etc-pyrrolidinone I and J (5), etc-pyrrolidinone C and D (6), etc-pyrrolidinone E (7), etc-pyrrolidinone F (8), etc-pyrrolidinone A (9), (-)-8-(5''S)-N-ethyl-2-pyrrolidinone-3-O-cinnamoylepicatechin (10), (-)-8-(5''R)-N-ethyl-2-pyrrolidinone-3-O-cinnamoylepicatechin (11), (-)-6-(5''S)-N-ethyl-2-pyrrolidinone-3-O-cinnamoylepicatechin (12), ECG, EGCG, CG, and GCG were separated and identified from teas in our laboratory and their purity was detected by HPLC (Fig. S1-2) (Cheng et al., 2018; Gaur et al., 2020; Li et al., 2018). Fig. 1 shows the chemical structures of the 16 tested tea catechins.

Molecular docking

Autodock 4.2 was used to study the interaction between catechins and 3CLpro. We obtained the crystal structure of the 3CLpro at 2.24 Å (code: 6LU7) from the Protein Data Bank. Before the docking process, we deleted all of the water molecules and co-crystallized ligand from the crystal structure of the 3CLpro. Then we used ChemBio3D 14.0 to optimize the 3D structure of the compounds based on the energy minimization. The grid points in the X, Y, and Z-axis were set at 50 × 55 × 50 Å with a grid point spacing of 0.375 Å. The grid center was placed in the active site pocket center at (-11.3, 13.5, 70.3). LGA runs were set at 100 (ga_run), with a population size (ga_pop_size) of 150, an energy evaluation (ga_num_evals) 25,000,000, and a maximum number of generations (ga_num_generations) 27,000. All other parameters were defaulted for AutoDock 4.2. PyMOL was used to visualize the docked pose of the compounds at the active site of the 3CLpro.

Establishment of intracellular model for detecting 3CLpro activity

Cell seeding and compounds dilution on day 1: we made 100 × compound solution in DMSO : H₂O (1:1), added 6 μl 100 × catechins to 54 μl growth medium, and diluted catechins with growth medium to 10 × final concentration. Cells (293T/17) were incubated for 20-24 h in a 60 mm petri dish.

Cell seeding on day 2: cells (293T/17) were transiently transfected with the 3CLpro activity detection system. After 6-8 h, the cells were centrifuged and suspended in a growth medium and then counted with a cell counter. Then we diluted the cell suspension in growth medium to the desired density, and 90 μl of the cell suspension was placed in a 96-well plate. Then we added 10 μl 10 × compounds to 96-well plates. The

final DMSO concentration in each well was 0.5%. The cells were incubated at 37 °C, 5% CO₂ for 16 h.

Measurement on day 3: we first equilibrated the microplate to room temperature. The concentration of each compound was 100, 10, and 1 μM. Then we assayed with 3CLpro activity detection system into each well and mixed it on an orbital shaker for 2 min to induce cell lysis. The mixture was cultivated at room temperature for 5 min to stabilize the luminescence signal. Finally, renilla luminescence (RLU) and fluminescence (Flu) was recorded on SpectraMax Paradigm (Molecular Devices, Sunnyvale, CA, USA). Inhibition (%) was calculated relative to the wells treated with the carrier (DMSO) using the following formula. Graphpad 7.0 software (San Diego, CA, USA) was used to analyze the data and fit it to a 4-parameter equation to generate a concentration-response curve.

Extracellular 3CLpro inhibition activity

We made a 100 × compound solution in DMSO : H₂O (1:1), added 4 μl 100 × compounds to 36 μl buffer, and diluted the compounds with growth medium to 10 × final concentration. We mixed 1 μl 3CLpro, 2 μl compounds, and 15 μl buffer (50 mM Tris, 1 mM EDTA) as the reaction system. The concentration of 3CLpro was 1400 μg/ml, and the compound concentrations were 0.015, 0.045, 0.14, 0.41, 1.24, 3.70, 11.10, 33.33, and 100 μM. Inhibition (%) was calculated relative to vehicle (DMSO) treated control wells using the following formula, and data were analyzed using Graphpad 7.0, fitting to a 4-parameter equation to generate concentration-response curves. We incubated the mixture at room temperature for 30 min and added substrate 2 μl to the mixture. We continued incubating the mixture at room temperature for 20 min and recorded renilla luminescence (Rlu) on SpectraMax Paradigm.

$$\%inhibition = RLU\ compound / RLU\ DMSO\ control * 100\%$$

Immobilization of 3CLpro on the chip surface

PBS-P buffer was selected as the coupling buffer, and 10 × PBS-P (pH 7.4) was diluted 10 times to prepare a 200 ml running buffer. 3CLpro was diluted to 10 μg/ml, with sodium acetate at pH 5.50, 5.00, 4.50, and 4.00, respectively, and 100 μl was prepared for each pH. Through a pre-enrichment experiment, pH 5.00 was determined as the best coupling condition. Therefore, the ligand solution was diluted to 10 μg/ml, with sodium acetate and pH 5.00. The formal coupling operation was carried out with 200 μl.

First, we injected a freshly prepared mixture of N-hydroxysuccinimide and N-ethyl-N'-(dimethylaminopropyl) carbodiimide (1:1 v/v) at a flow rate of 10 μl/min for 420 s to activate the CM7 chip. Next, we injected the 3CLpro, at a concentration of 10 μg/ml in immobilization buffer (10 mM sodium acetate at pH 5.00) into the sample channel and allowed the 3CLpro to react the CM7 chip for 7 min at a flow rate of 10 μl/min, resulting in 3CLpro immobilized densities averaging 4000 RU. At last, we injected a solution of ethanolamine hydrochloride at pH 4.50 at a flow rate of 10 μl/min to block the remaining carboxyl groups.

Analysis of compounds interactions with immobilized 3CLpro

For the interaction experiments, the solutions of compounds were prepared in 1 × PBS-P buffer used in the interaction between protein and

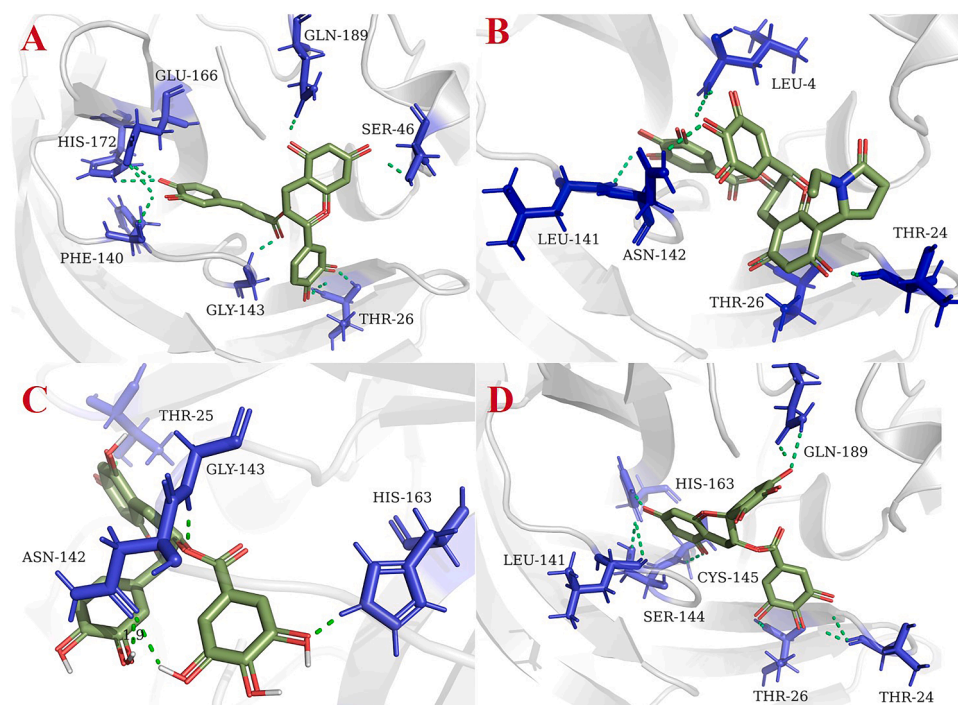


Fig. 2. Interactions of four active catechins with 3CL protease with 3D docking mode, showing that (-)-epicatechin 3-O-caffeate (1), etc-pyrrolidinone C and D (6), (-)-epicatechin gallate (ECG), and (+)-gallocatechin gallate (GCG) interacts with the key binding residues of 3CL protease.

catechins. We analyzed a range of concentrations (0.39, 0.78, 1.56, 3.13, 6.25, 12.50, 25.00 μM) to obtain the sensorgrams of the interactions between 3CLpro and the catechins. The catechins were injected onto the 3CLpro immobilized chip for 180 s at a flow rate of 20 $\mu\text{L}/\text{min}$ and $1 \times \text{PBS-P}$ buffer was injected for 160 s at a flow rate of 20 $\mu\text{L}/\text{min}$ to regenerate the chip surface at the end of each experiment. Sensorgrams were processed by using automatic correction for nonspecific bulk refractive index effects. The equilibrium dissociation constants (K_D) evaluating the 3CLpro-catechins binding affinity were determined by the steady-state affinity fitting analysis of the Biacore data by using Biacore T200 Evaluation software (Liu et al., 2021).

Statistical analysis

All data were analyzed using one-way ANOVA, followed by multiple tests. The results were expressed as mean values \pm standard deviations. GraphPad Prism (version 8.0) software was applied for statistical analysis.

Results

Molecular docking and interaction analysis

The molecular docking was assessed by binding constant (K_i) and binding energy (E_a). A lower value of K_i and E_a indicates that the compound can bind to 3CLpro more tightly (Bhardwaj et al., 2021). Table S1 lists the E_a and K_i values. Molecular docking results showed that all catechins can bind 3CLpro, suggesting that these catechins have potential 3CLpro inhibitory effects. The possible binding sites where 3CLpro interacted with catechins were drawn by PyMol. The binding sites of EC-C (1) are at Thr26, Ser46, Phe140, Gly143, Glu166, His172, Gln189, and those of etc-pyrrolidinone C and D (6) are at Leu4, Thr24, Thr26, Leu141, Asn142. ECG interacts with 3CLpro at Thr25, Asn142, Gly143, His163. GCG interacts with 3CLpro at the sites of Thr24, Thr26, Cys145, Ser144, Leu141, His163, Gln189. Their K_i values are 21.71 (1), 172.45 (6), 28.79 (ECG), 14.34 (GCG) nM and E_a were -10.45 (1), -9.23 (6), -10.29 (ECG), -10.21 (GCG) kcal/mol. The complexes of 3CLpro and

catechins suggest that the residues Thr24, Thr26, Asn142, Gly143, His163, and Gln189 are the key amino acids for the interaction between the catechins and 3CLpro (Guo et al., 2021; Sabbah et al., 2021).

Intracellular 3CLpro inhibition of selected catechins

To understand the inhibition of these docking promising catechins against 3CLpro, we used 16 tea catechins obtained from our group. Their purity was detected by HPLC (Fig. S1-2) (Cheng et al., 2018; Gaur et al., 2020; Ke et al., 2019; Li et al., 2018; Wang et al., 2021) including the known major tea catechins ECG, EGCG, CG and GCG to perform intracellular inhibition assay. Ebselen [(2-phenyl-1, 2-benzisoxazol-3 (2H)-one)] was used as the positive control ($\text{IC}_{50} = 69.70 \pm 0.28 \text{ nM}$). Except for compounds zijuanin D (3) and (-)-8-(5'-R)-N-ethyl-2-pyrrolidinone-3-O-cinnamoylepicatechin (11), other catechins showed dose-dependent inhibition against 3CLpro (Fig. 3, Fig. S3-S5). When the concentration is 100 μM , ECC (1), etc-pyrrolidinone C and D (6), ECG, and GCG have stronger intracellular 3CLpro inhibition (with the ratios at 93.55 ± 0.06 , 93.66 ± 0.14 , 79.69 ± 1.70 , $93.56 \pm 0.04 \%$, respectively) than others.

Extracellular 3CLpro inhibition

The IC_{50} values for EC-C (1), zijuanin C (2), etc-pyrrolidinone C and D (6), etc-pyrrolidinone F (8), GCG, and ECG were 1.58 ± 0.21 , 41.20 ± 3.56 , 0.90 ± 0.03 , 46.71 ± 10.50 , 3.38 ± 0.48 , and $71.78 \pm 8.36 \mu\text{M}$ (Fig. 4, Fig. S6-8), respectively. IC_{50} values of other compounds are higher than 100 μM . The IC_{50} of the positive drug ebselen is $40.00 \pm 0.40 \text{ nM}$. Three compounds (1, 6, and GCG) have IC_{50} values less than 10 μM (Fig. 4). This extracellular result is consistent with that of the intracellular one.

Surface plasmon resonance (SPR) analysis

To obtain the dissociation constants between 3CLpro and catechins, SPR data have been analyzed by fitting the SPR sensorgrams using non-linear fitting of the SPR signal at the steady-state with a Langmuir

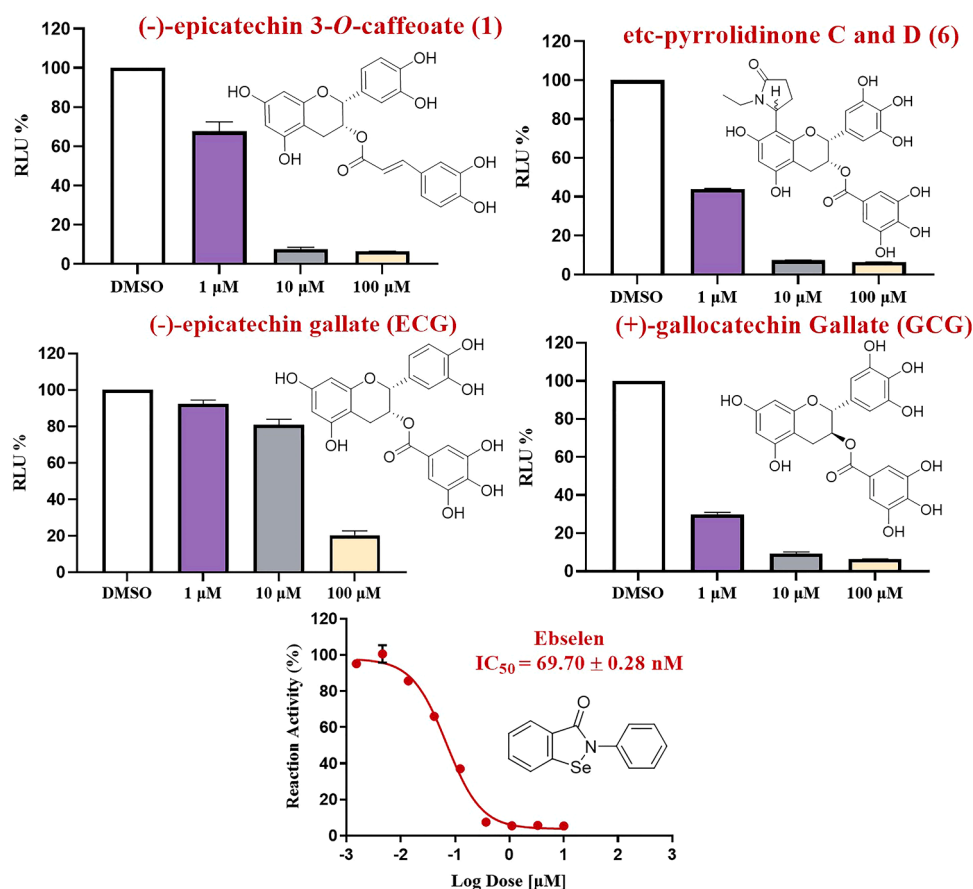


Fig. 3. Intracellular inhibition of (-)-epicatechin 3-O-caffeate (1), etc-pyrrolidinone C and D (6), (-)-epicatechin gallate (ECG), and (+)-gallocatechin gallate (GCG) against SARS-CoV-2 3CL protease activity. Data are means \pm SD from three experiments. Ebselen [(2-phenyl-1, 2-benzoselenazol-3(2H)-one)] was used as the positive control ($IC_{50} = 69.70 \pm 0.28$ nM), Z-factor = 0.83.

binding isotherm model. Five concentration gradients of each analyte were plotted with the response value at equilibrium. Rmax is the maximum response value. Offset is the minimum response value. The

fitting efficiency is calculated by the χ^2 value. Table S2 shows that EC-C (1), etc-pyrrolidinone C and D (6), and GCG have low K_D values (4.29, 3.46, and 3.63 μM, respectively) (Fig. 5), indicating that they all have

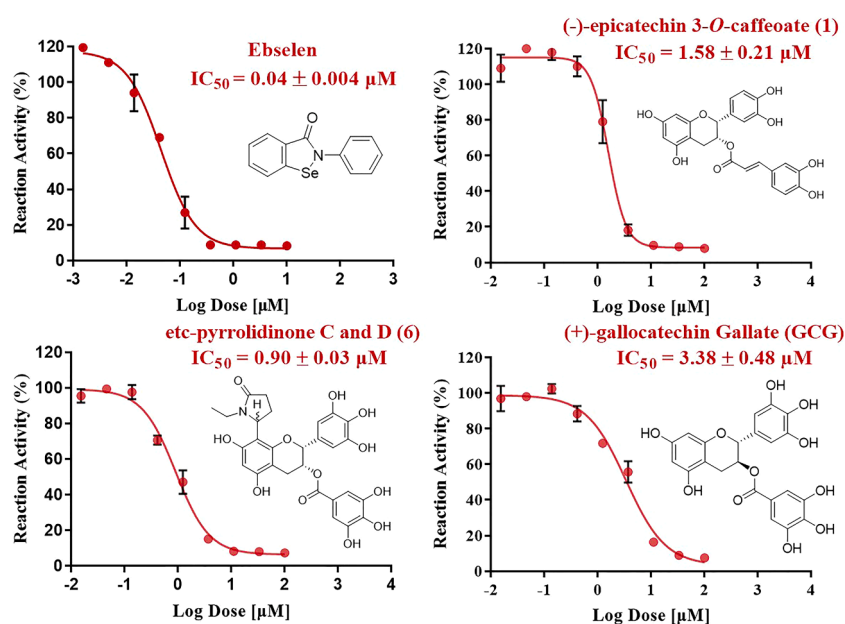


Fig. 4. Extracellular Inhibition of ebselen, (-)-epicatechin 3-O-caffeate (1), etc-pyrrolidinone C and D (6), and (+)-gallocatechin gallate (GCG) against SARS-CoV-2 3CL protease activity. Data are means \pm SD from three experiments. The IC_{50} of the positive drug ebselen is 40.00 ± 0.40 nM.

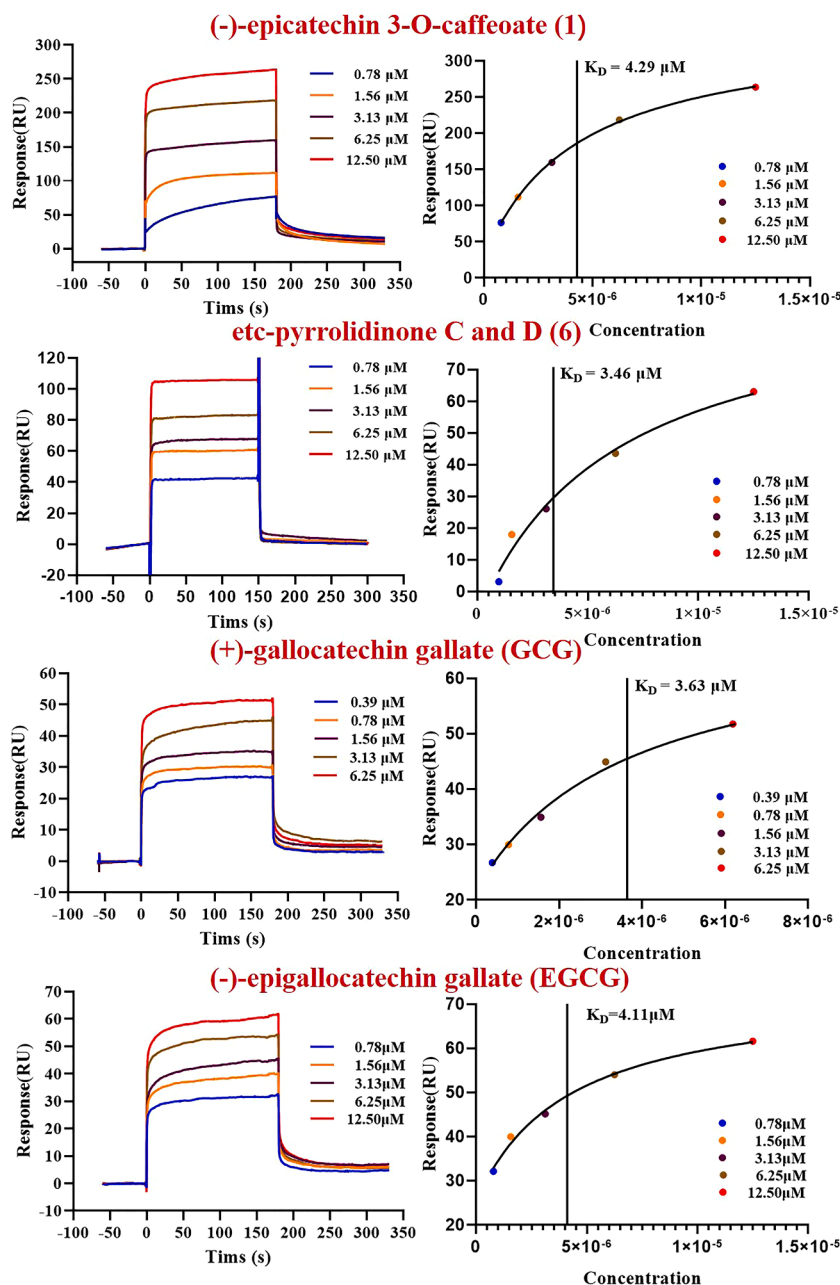


Fig. 5. Sensorgrams for (-)-epicatechin 3-O-caffeate (1) (0.78–12.50 μM), etc-pyrrolidinone C and D (6) (0.78–12.50 μM), (+)-gallocatechin gallate (GCG) (0.39–6.25 μM), (-)-epigallocatechin gallate (EGCG as the positive control) (0.39–6.25 μM) flowing over a CM7 3CL protease-immobilized sensor-chip surface at 25°C. Steady-state affinity analysis of (-)-epicatechin 3-O-caffeate (1), etc-pyrrolidinone C and D (6), and (+)-gallocatechin gallate (GCG) binding to 3CL protease was fitted to a 1:1 interaction model.

strong 3CLpro binding affinity. EGCG was used as the positive control with K_D value at 4.11 μM (Fig. 5). The lower calculated χ^2 value indicates a good accuracy of the fitting. This means that these catechins can bind 3CLpro tightly.

Discussion

Searching for leading natural products from functional food is always a safe and attractive approach for the prevention, alleviation, and treatment of human diseases. Tea, as a traditional safe drink containing amounts of polyphenols, has various antiviral activities (Gaur and Bao, 2021). Specifically, green tea has anti-SARS-CoV-2 and 3CLpro inhibition effects (Upadhyay et al., 2020), suggesting that green tea could be an effective resource for searching and subsequent designing 3CLpro inhibitors against the contagious virus.

We selected 16 catechins for molecular docking with 3CLpro (Table S1). The molecular docking results suggest that these tea

catechins could be potential 3CLpro inhibitors. However, the binding sites of catechins at 3CLpro are different although they are in the same pocket (Fig. 2). EC-C (1) interacts with the protein through ten hydrogen bonds at Thr26, Gly143, Phe140, His172, Glu166, Gln189, and Ser46. 3CLpro binds etc-pyrrolidinone C and D (6) through six hydrogen bonds at Leu4, Thr24, Thr26, Leu141, Asn142. ECG interacts with 3CLpro through five hydrogen bonds at Thr25, Asn142, Gly143, His163 while GCG interacts with it through ten hydrogen bonds at the sites of Thr24, Thr26, Cys145, Ser144, Leu141, His163, Gln189. Previous studies found His41, Gly143, Ser144, Cys145, His163, and Glu166 make contributions to interact with small molecular ligands through hydrogen bonds (Sabbah et al., 2021). Together, the dominant residue of 3CLpro does provide theoretical guidance for further design of molecules with greater binding capacity and stronger inhibitory abilities.

Previous studies suggest that galloyl substitution is critical for 3CLpro inhibition of tea catechins and theaflavins (Henss et al., 2021; Zhu and Xie, 2020). EC-C (1) is a bioactive catechin derivative with a

caffeoyl group substituted at 3-OH other than a normal galloyl substitution at 3-OH such as those of ECG or EGCG. Our previous studies showed that this caffeoyl substitution enhanced its bioactivities (Wang et al., 2017; Zhang et al., 2018), which is consistent with the present result (Fig. 3, Fig. S3-5).

Previous studies also suggest that additional hydroxyl groups at the B ring might enhance catechins' protein binding capacity (Liu et al., 2021). Although the present study did not show this trend with a stronger inhibition of ECG ($IC_{50} = 71.78 \pm 8.36 \mu M$) than that of EGCG ($IC_{50} > 100 \mu M$) (Fig. S8), it is consistent with the α -amylase inhibition activity in which that the catechol-type catechins were stronger than the pyrogallol-type catechins (Xiao et al., 2013).

Zijuanin C (2) and zijuanin D (3) (C-3'' isomers), (-)-8-(5''S)-N-ethyl-2-pyrrolidinone-3-O-cinnamoylepicatechin (10) and (-)-8-(5''R)-N-ethyl-2-pyrrolidinone-3-O-cinnamoylepicatechin (11) (C-5'' isomers) are stereoisomers (Fig. 1), among which 2 and 10 can inhibit 3CLpro, while 3 and 11 cannot, suggesting that the stereoisomers of these catechins do affect their activities. Similarly, the activity of GCG ($IC_{50} = 3.38 \pm 0.48 \mu M$) is far stronger than its isomer EGCG, which is consistent with previous studies (Nguyen et al., 2012; Zhu and Xie, 2020). Importantly, heating is an important processing procedure for tea production, which can lead to transforming EGCG to GCG (Zhou et al., 2018) and other important catechins (Zhang et al., 2021), thus enhancing various bioactivities of tea (Zhou et al., 2018) as well as the potential SARS-CoV-2 inhibition.

Although the major tea catechin EGCG showed weaker 3CLpro inhibition, it was reported to inhibit SARs-CoV-2 infections through different mechanisms (Henss et al., 2021; Zhang et al., 2021). Severe SARs-CoV-2 infection and high mortality are mainly caused by cytokine storm and inflammation, triggering a huge burden of oxidative imbalance on the immune system (El-Missiry et al., 2020; Zhang et al., 2021). As such, antioxidant, anti-inflammatory and immunity-enhancing therapies have become promising approaches to effectively treat COVID-19, contributed greatly by Traditional Chinese Medicine in China (Li et al., 2020). Various tea products (green, black, oolong, and roasted teas) contain lines of polyphenols. The major tea catechins EGCG, theasinensin A, and gallated theaflavins exhibit viral prophylactic effects possibly through maintaining the redox homeostasis (Bao et al., 2013; El-Missiry et al., 2020; Ohgitani et al., 2021).

Our above results and structure-activity relationship analyses suggest that the 2-ethylpyrrolidinone substitution (such as the flavoalkaloids 4-9 vs. ECG and EGCG, Fig. 1) might not improve the 3CLpro inhibition activity. The different ester substitution (galloyl and cinnamoyl) of 3-OH strongly improved this activity, which might come from the large number of hydrogen bonds contributed by the hydroxyl groups at the ester substitute (ten each for EC-C and GCG). The changes in the configuration of C-3, C-3'', and C-5'' could also affect the 3CLpro inhibition activity, which could make the molecules easily enter into the protein. Our present study provided some tea catechins with small 3CLpro IC_{50} values, suggesting that structural modification at these positions of catechins might be a promising approach to discover new small molecular SARS-CoV-2 inhibitors from tea.

Limitations of the present study are also apparent: first, we only check the inhibition assays at a protein level, not real anti-viral assays; second, the correlation between tea consumption and inhibition of SARS-CoV-2 infection is not clear yet. Therefore, further researches could be conducted on the *in vitro* and *in vivo* antiviral activities of these active catechins for their realistic application. We can expect the use of tea consumption as prophylactic antioxidant supplementation to enhance the antioxidant, anti-inflammatory effects, and further immune booster, other than direct antiviral therapy.

Conclusion

Docking results suggested that 3CLpro interacted with the selected 16 catechins with low binding energy through the key amino acid

residues Thr24, Thr26, Asn142, Gly143, His163, and Gln189. The 3CLpro activity detection system showed that these catechins except 3 and 11 can inhibit 3CLpro activity intracellularly, among which EC-C (1), etc-pyrrolidinone C and D (6), ECG, and GCG showed stronger inhibition. The extracellular 3CLpro IC_{50} values of 1, zijuanin C (2), etc-pyrrolidinone C and D (6), etc-pyrrolidinone F (8), GCG, and ECG are $1.58 \pm 0.21 \mu M$, $41.2 \pm 3.56 \mu M$, $0.90 \pm 0.03 \mu M$, $46.71 \pm 10.50 \mu M$, $3.38 \pm 0.48 \mu M$, and $71.78 \pm 8.36 \mu M$, respectively. The K_D values determined by SPR are $4.29 \mu M$ for 1, $3.46 \mu M$ for 6, and $3.36 \mu M$ for GCG. Our results indicate that the ester substitution of 3-OH and the configurations at position C-3, C-3'', and C-5'' could affect the 3CLpro inhibition activity, suggesting that further structural modification could be conducted at 3-OH as well as the configuration changes at C-3, C-3'', and C-5''.

Author Contributions

G.-H.B. and S.-Y.L. designed the experiments. S.-Y.L. and W.W. did most of the experiments. G.-H.B., J.-P.K., and P. Z. did some experiments. S.-Y.L. and G.-H.B. wrote the paper. G.-X.C. and G.-H.B. contribute to funding acquisition.

Declaration of Competing Interest

We wish to draw the attention of the Editor to the following facts which may be considered as potential conflicts of interest and to significant financial contributions to this work.

Guan-Hu Bao reports financial support was provided by National Natural Science Foundation of China. Guan-Hu Bao has patent #a new 3CL protease inhibitor preparation and use thereof CN202110687240.3 pending to China Patent.

Acknowledgments

We got great help from PreceDo Pharmaceuticals Co. Ltd (Hefei, China) for 3CLpro preparation and transfected 293T/17 cells.

Funding

This work was supported by The Open Fund of State Key Laboratory of Tea Plant Biology and Utilization [grant number SKLTOF2018011] and National Natural Science Foundation of China [grant number 31972462; U19A2034].

Supplementary materials

Supplementary material associated with this article can be found, in the online version, at doi:10.1016/j.phymed.2021.153853.

References

- Bao, G.H., Xu, J., Hu, F.L., Wan, X.C., Deng, S.X., Barasch, J., 2013. EGCG inhibit chemical reactivity of iron through forming an Ngal-EGCG-iron complex. *Biomaterials* 26, 1041–1050. <https://doi.org/10.1007/s10534-013-9681-8>.
- Bhardwaj, V. K., Singh, R., Sharma, J., Rajendran, V., Purohit, R. and Kumar, S. 2021. Bioactive Molecules of Tea as Potential Inhibitors for RNA-Dependent RNA Polymerase of SARS-CoV-2. *Front Med.* 8, 645. <https://doi.org/10.3389/fmed.2021.684020>.
- Cheng, J., Wu, F.H., Wang, P., Ke, J.P., Wan, X.C., Qiu, M.H., Bao, G.H., 2018. Flavoalkaloids with a pyrrolidinone ring from Chinese ancient cultivated Tea Xi-Gui. *J. Agric. Food Chem.* 66, 7948–7957. <https://doi.org/10.1021/acs.jafc.8b02266>.
- El-Missiry, M.A., Fekri, A., Kesar, L.A., Othman, A.I., 2020. Polyphenols are potential nutritional adjuvants for targeting COVID-19. *Phytother. Res.* 35, 2879–2889. <https://doi.org/10.1002/ptr.6992>.
- Gaur, R., Bao, G.H., 2021. Chemistry and pharmacology of natural catechins from *Camellia sinensis* as anti-MRSA agents. *Curr. Top. Med. Chem.* 21, 1519–1537. <https://doi.org/10.2174/1568026621666210524100632>.
- Gaur, R., Ke, J.P., Zhang, P., Yang, Z., Bao, G.H., 2020. Novel cinnamoylated flavoalkaloids identified in tea with acetylcholinesterase inhibition effect. *J. Agric. Food Chem.* 68, 3140–3148. <https://doi.org/10.1021/acs.jafc.9b08285>.

- Grottesi, A., Bešker, N., Emerson, A., Manelfi, C., Beccari, A.R., Frigerio, F., Lindahi, E., Cerchia, C., Talarico, C., 2020. Computational studies of SARS-CoV-2 3CLpro: Insights from MD simulations. *Int. J. Mol. Sci.* 21, 5346. <https://doi.org/10.3390/ijms21155346>.
- Henss, L., Auste, A., Schürmann, C., Schmidt, C., von Rhein, C., Mühlebach, M.D., Schnierle, B.S., 2021. The green tea catechin epigallocatechin gallate inhibits SARS-CoV-2 infection. *J. Gen. Virol.* 102, 001574. <https://doi.org/10.1099/jgv.0.001574>.
- Jang, M., Park, R., Park, Y.I., Cha, Y.E., Yamamoto, A., I.L., J., Park, J., 2021. EGCG, a green tea polyphenol, inhibits human coronavirus replication in vitro. *Biochem. Biophys. Res. Comm.* 547, 23–28. <https://doi.org/10.1016/j.bbrc.2021.02.016>.
- Ke, J.P., Dai, W.T., Zheng, W.J., Wu, H.Y., Hua, F., Hu, F.L., Chu, G.X., Bao, G.H., 2019. Two pairs of isomerically new phenylpropanoidated epicatechin gallates with neuroprotective effects on H2O2-injured SH-SY5Y cells from Zijuan Green tea and their changes in fresh tea leaves collected from different months and final product. *J. Agric. Food Chem.* 67, 4831–4838. <https://doi.org/10.1021/acs.jafc.9b01365>.
- Kim, Y., Liu, H.K., Galasiti, A.C., Weerasekara, S., Hua, D.H., Groutas, W.C., Chang, K.O., Pedersen, N.C., 2016. Reversal of the progression of fatal coronavirus infection in cats by a broad-spectrum coronavirus protease inhibitor. *Plos Pathog* 12, e1005650. <https://doi.org/10.1371/journal.ppat.1005650>.
- Li, C., Wang, L., Ren, L., 2020. Antiviral mechanisms of candidate chemical medicines and traditional Chinese medicines for SARS-CoV-2 infection. *Virus Res* 286, 198073. <https://doi.org/10.1016/j.virusres.2020.198073>.
- Li, Q., Guan, X.H., Wu, P., Wang, X.Y., Zhou, L., Tong, Y.Q., Ren, R.Q., Leung, K.S.M., Lau, E.H.Y., Wong, J.Y., Xing, X.S., Xiang, N.J., Wu, Y., Li, C., Chen, Q., Li, D., Liu, T., Zhao, J., Liu, M., Tu, W.X., Chen, C.D., Jin, L.M., Yang, R., Wang, Q., Zhou, S. H., Wang, R., Liu, H., Luo, Y.B., Liu, Y., Shao, G., Li, H., Tao, Z.F., Yang, Y., Deng, Z. Q., Liu, B.X., Ma, Z.T., Zhang, Y.P., Shi, G.Q., Lam, T.T.Y., Wu, J.T., Gao, G.F., Cowling, B.J., Yang, B., Leung, G.M., Feng, Z.J., 2020. Early transmission dynamics in Wuhan, China, of novel coronavirus-infected pneumonia. *New Engl. J. Med.* 382, 1199–1207. <https://doi.org/10.1056/NEJMoa2001316>.
- Liu, S.Y., Zhang, Y.Y., Chu, G.X., Bao, G.H., 2021. N-ethyl-2-pyrrolidinone substitution enhances binding affinity between tea flavoalkaloids and human serum albumin: Greatly influenced by esterization. *Spectrochim. Acta. A Mol. Biomol. Spectrosc.* 262, 120097. <https://doi.org/10.1016/j.saa.2021.120097>.
- Li, X., Liu, G.J., Zhang, W., Zhou, Y.L., Ling, T.J., Wan, X.C., Bao, G.H., 2018. Novel flavoalkaloids from white tea with inhibitory activity against the formation of advanced glycation end products. *J. Agric. Food Chem.* 66, 4621–4629. <https://doi.org/10.1021/acs.jafc.8b00650>.
- Nguyen, T.T.H., Woo, H.J., Kang, H.K., Nguyen, V.D., Kim, Y.M., Kim, D.W., Ahn, S.A., Xia, Y., Kim, D., 2012. Flavonoid-mediated inhibition of SARS coronavirus 3C-like protease expressed in *Pichia pastoris*. *Biotechnol. Lett.* 34, 831–838. <https://doi.org/10.1007/s10529-011-0845-8>.
- Nishimura, H., Okamoto, M., Daput, I., Katumi, M., Oshitani, H., 2021. Inactivation of SARS-CoV-2 by Catechins from Green Tea. *Jpn. J. Infect. Dis.* 74, 421–423. <https://doi.org/10.7883/yoken.jjid.2020.902>.
- Oberfeld, B., Achanta, A., Carpenter, K., Chen, P., Gillette, N.M., Langat, P., Said, J.T., Schiff, A.E., Zhou, A.S., Barczak, A.K., Pillai, S., 2020. SnapShot: COVID-19. *Cell* 181, 954. <https://doi.org/10.1016/j.cell.2020.04.013>.
- Ohgita, E., Shin-Ya, M., Ichitani, M., Kobayashi, M., Takihara, T., Kawamoto, M., Kinugasa, H., Mazda, O., 2021. Significant inactivation of SARS-CoV-2 by a green tea catechin, a catechin-derivative and galloylated theaflavins in vitro. *Molecules* 26, 3572. <https://doi.org/10.3390/molecules26123572>.
- Sabbah, D., Hajjo, R., Bardaweel, S., Zhong, H., 2021. An updated review on betacoronavirus viral entry inhibitors: Learning from past discoveries to advance COVID-19 drug discovery. *Curr. Top. Med. Chem.* 21, 571–596. <https://doi.org/10.2174/1568026621666210119111409>.
- Sharma, J., Kumar, V., Singh, R., Rajendran, V., Purohit, R., Kumar, S., 2021. An in-silico evaluation of different bioactive molecules of tea for their inhibition potency against non structural protein-15 of SARS-CoV-2. *Food Chem* 346, 128933. <https://doi.org/10.1016/j.foodchem.2020.128933>.
- Upadhyay, S., Tripathi, P.K., Singh, M., Raghavendhar, S., Bhardwaj, M., Patel, A.K., 2020. Evaluation of medicinal herbs as a potential therapeutic option against SARS-CoV-2 targeting its main protease. *Phytother. Res.* 34, 3411–3419. <https://doi.org/10.1002/ptr.6802>.
- Wang, W., Fu, X.W., Dai, X.L., Hua, F., Chu, G.X., Chu, M.J., Hu, F.L., Ling, T.J., Gao, L. P., Xie, Z.W., Wan, X.C., Bao, G.H., 2017. Novel acetylcholinesterase inhibitors from Zijuan tea and biosynthetic pathway of caffeoylated catechin in tea plant. *Food Chem* 237, 1172–1178. <https://doi.org/10.1016/j.foodchem.2017.06.011>.
- Wang, W., Zhang, P., Liu, X.H., Ke, J.P., Zhuang, J.H., Ho, C.T., Xie, Z.W., Bao, G.H., 2021. Identification and quantification of hydroxycinnamoylated catechins in tea by targeted UPLC-MS using synthesized standards and their potential use in discrimination of tea varieties. *LWT - Food Sci. Technol.* 142, 110963. <https://doi.org/10.1016/j.lwt.2021.110963>.
- Wet, J.D., Wood, K.V., Helinski, D.R., Deluca, M., 1986. Cloning of firefly luciferase cDNA and the expression of active luciferase in *Escherichia coli*. *PNAS* 82, 7870–7873. <https://doi.org/10.1073/pnas.82.23.7870>.
- Williams, T.M., Burlein, J.E., Ogden, S., Kricka, L.J., Kant, J.A., 1989. Advantages of firefly luciferase as a reporter gene: application to the interleukin-2 gene promoter. *Anal. Biochem.* 176, 28–32. [https://doi.org/10.1016/0003-2697\(89\)90267-4](https://doi.org/10.1016/0003-2697(89)90267-4).
- Xiao, J., Ni, X., Kai, G., Chen, X., 2013. A review on structure–activity relationship of dietary polyphenols inhibiting α -Amylase. *Crit. Rev. Food Sci.* 53, 497–506. <https://doi.org/10.1080/10408398.2010.548108>.
- Zhang, P., Wang, W., Liu, X.-H., Yang, Z., Gaur, R., Wang, J.-J., Ke, J.-P., Bao, G.-H., 2021. Detection and quantification of flavoalkaloids in different tea cultivars and during tea processing using UPLC-TOF-MS/MS. *Food Chem* 339, 127864. <https://doi.org/10.1016/j.foodchem.2020.127864>.
- Zhang, W., Li, X., Hua, F., Chen, W., Wang, W., Chu, G.X., Bao, G.H., 2018. Interaction between ester-type tea catechins and neutrophil gelatinase-associated lipocalin: inhibitory mechanism. *J. Agric. Food Chem.* 66, 1147–1156. <https://doi.org/10.1021/acs.jafc.7b05399>.
- Zhang, Z., Zhang, X., Bi, K., He, Y., Yan, W., Yang, C.S., Zhang, J., 2021. Potential protective mechanisms of green tea polyphenol EGCG against COVID-19. *Trends Food Sci. Technol.* 114, 11–24. <https://doi.org/10.1016/j.tifs.2021.05.023>.
- Zhou, J., Zhang, L., Meng, Q., Wang, Y., Long, P., Ho, C.T., Cui, C., Cao, L., Li, D., Wan, X., 2018. Roasting process improves the hypoglycemic effect of large-leaf yellow tea infusion by enhancing levels of the epimerized catechins that inhibit α -glucosidase. *Food Funct* 9, 5162–5168.
- Zhu, Y., Xie, D.Y., 2020. Docking Characterization and in vitro Inhibitory Activity of Flavan-3-ols and Dimeric Proanthocyanidins against the main protease activity of SARS-Cov-2. *Front. Plant Sci* 11, 601316. <https://doi.org/10.3389/fpls.2020.601316>.